Prepared for submission to JINST

Magneto-optic probe measurements in low density-supersonic jets

M. Oliver,[a,1] **T. White,**[a] **P. Maybe,**[a] **M. Kühn-Kauffeldt,**[b] **L. Döhl,**[c] **R. Bingham,**[d,e] **R. Clarke,**[d] **P. Graham,**[f] **R. Heathcote,**[d] **M. Koenig,**[g] **Y. Kuramitsu,**[h] **D. Q. Lamb,**[i] **J. Meinecke,**[a] **T. Michel,**[g] **F. Miniati,**[j] **M. Notley,**[d] **B. Reville,**[k] **S. Sarkar,**[a] **Y. Sakawa,**[l] **A. A. Schekochihin,**[a] **P. Tzeferacos,**[i] **N. Woolsey,**[c] **H.-S. Park,**[m] **and G. Gregori**[a]

[a] *University of Oxford,*
Clarendon Laboratory, Parks Road, Oxford OX1 3PU, UK
[b] *Universität der Bundeswehr,*
München, Neubiberg, Germany
[c] *Department of Physics University of York,*
Heslington, York, YO10 5DD, UK
[d] *Rutherford Appleton Laboratory,*
Chilton, Didcot, OX11 0QX, UK
[e] *Department of Physics,*
University of Strathclyde, Glasgow, G4 0NG, UK
[f] *AWE,*
Aldermaston, Reading, West Berkshire, RG7 4PR, UK
[g] *Laboratoire pour lâĂŹUtilisation de Lasers Intenses,*
UMR7605, CNRS CEA, Université Paris VI Ecole Polytechnique, 91128 Palaiseau Cedex, France
[h] *National Central University,*
Taoyuan, Taiwan
[i] *Department of Astronomy and Astrophysics,*
University of Chicago, 5640 S. Ellis Ave, Chicago, IL 60637, USA
[j] *ETH Zurich,*
Zurich, Switzerland
[k] *School of Mathematics and Physics,*
Queens University Belfast, Belfast BT7 1NN, UK
[l] *Institute of Laser Engineering,*
Osaka, Japan
[m] *Lawrence Livermore National Laboratory,*
California, USA

E-mail: matthew.oliver@physics.ox.ac.uk

[1] Corresponding author.

Abstract: A magneto-optic probe was used to make time-resolved measurements of the magnetic field in both a single supersonic jet and in a collision between two supersonic turbulent jets, with an electron density $\approx 10^{18}$ cm^{-3} and electron temperature ≈ 4 eV. The magneto-optic data indicated the magnetic field reaches $B \approx 200$ G. The measured values are compared against those obtained with a magnetic induction probe. Good agreement of the time-dependent magnetic field measured using the two techniques is found.

Keywords: Plasma diagnostics - probes, Lasers

Contents

1 Introduction

Magnetic fields play an important role in plasma dynamics and particle acceleration in astrophysics [1–6]. This has led, in the past decade, to a wide range of laboratory experiments aimed at examining the amplification, structure, and dissipation of these fields [7–12]. Clearly, the understanding of the property of the magnetic fields in plasma require accurate diagnostics. The magnetic induction (B-dot) probe is a practical, accurate and sensitive instrument, able to make well-resolved field measurements [13]. However, this comes with several drawbacks. First of all, the B-dot is a mechanical probe that must be inserted into the plasma. This inevitably perturbs the properties of the plasma. To compensate for this, the probe must be miniaturized, such that its linear dimensions are smaller than the relevant spatial scales of interest. This poses several constraints on its construction, as a suitable B-dot probe for use in laboratory astrophysics experiments requires a bandwidth which is fast enough to resolve the dynamics of the flow [13].

Because of this, optical diagnostics may be advantageous. While the Zeeman effect, for example, offers an entirely non-invasive method of measuring the field, the spectral line splitting for typical plasma conditions in these experiments is of the order of other line broadening mechanisms, such as Doppler or Stark broadening[14, 15]. Considering an emission line with wavelength $\lambda = 400$ nm, a $B = 200$ G field gives and induced broadening due to Zeeman $\frac{\Delta\lambda}{\lambda} \sim 10^{-4}$, far smaller than the Doppler broadening at electronvolt temperatures. Faraday rotation of a probe laser is another commonly used technique for the measurements of magnetic fields [16]. However, for optical wavelengths, this requires the product of the magnetic field and plasma density to be large enough, typically requiring electron plasma densities $n_e \gtrsim 10^{18}$ cm^{-3} for an appreciable rotation. For instance in a 1 cm long plasma with a uniform electron density of $n_e = 10^{18}$ cm^{-3} and a uniform magnetic field $B = 200$ G, as in the experiment discussed in this paper, the change in the polarization rotation angle for a 532 nm probe beam would be less than 0.001° [16], which is challenging to measure. Alternatively, the Hanle effect, due to the depolarization of scattered light in atomic transitions involving magnetic sublevels, may also be used to measure fields in turbulent plasma. This has been applied to diagnose magnetic fields in the solar atmosphere[17]. The Hanle effect has the advantage that, while the Faraday rotation cancels out on average in a turbulent magnetic

field, the depolarization does not. However, when considering laboratory plasma conditions, for $n_e \sim 10^{18}$ cm^{-3}, it produces a measurable signal only for fields $B > 1$ kG[18].

In presence of smaller magnetic fields, Faraday rotation measurements are still possible, but they require the use of a small birefringent crystal placed within the plasma to increase the rotation. Magneto-optical probes, relying on this enhancement of the Faraday rotation, have been tested with large current-driven magnetic fields [19–21]. However, to our knowledge, they have not yet been used to measure smaller fluctuating magnetic fields within a plasma, nor tested against other diagnostics methods. Here, we discuss the results of an experiment aimed at measuring the magnetic field in a turbulent plasma. We compare the results from a magneto-optic probe to the measurements obtained with a B-dot probe.

As for the usual Faraday rotation, the magnitude of the rotation inside the birefringent crystal depends on the line integral of the component of the magnetic field along the laser path. As the electron density is constant in the crystal, the rotation angle, Φ, of an electromagnetic wave traveling along the axis of the crystal is given by

$$\Delta\Phi = V \int B(l) dl, \tag{1.1}$$

where V is known as the Verdet constant, $B(l)$ is longitudinal component of the magnetic field, and l is the length of the crystal. We used a terbium gallium garnet (TGG) crystal [22], which has $V = 190$ rad/T $\cdot$ m at $\lambda = 532$ nm, the wavelength of probe laser used in our experiment. The average field along the length of the crystal (L) is therefore

$$\langle B \rangle = \Delta\Phi / VL. \tag{1.2}$$

The probe beam was linearly polarized before entering the crystal and split by a 50/50 beam-splitter after passing through the crystal. The polarization of light after the crystal is given simply by

$$\Phi = \arctan \sqrt{\frac{\epsilon I_s}{I_p}}, \tag{1.3}$$

where I_s and I_p are the intensities of the two orthogonal polarizations, and ϵ is a factor accounting for different losses in each polarization due to losses in the optical pass and varying detector response. The factor ϵ is found by setting $\epsilon I_s = I_p$ when no magnetic field is present.

2 Experimental Setup

Both the Verdet crystal and B-dot probes were used as part of an experiment on supersonic turbulence performed at the Rutherford Appleton Laboratory (UK). The experimental setup is shown in Figure 1. The experiment consisted in creating two counter-propagating supersonic jets. Each jet was produced by firing three 2 ns long, $\approx$ 100 J, 527 nm, 200 μm diameter focal spot drive beams onto a 10 μm thick fluorinated plastic (PVDF) target inside of a vacuum chamber at an ambient pressure of $\approx 10^{-5}$ mbar. The jet passed through the central hole of a 5 kG ring magnet with a field parallel to the direction of the flow. The field was advected with the flow, which in the case of the

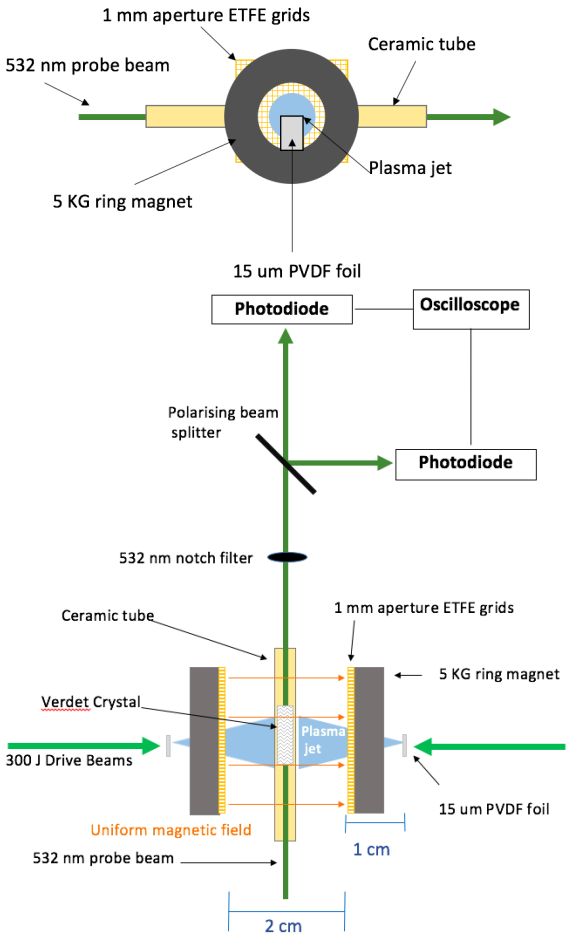

Figure 1. (a) View of the target from the direction of incoming drive beam. The target is ablated creating a plasma jet which advects the field of the ring magnet and becomes turbulent as it passes through the grid. (b) Top-down view of target and magneto-optic probe setup. Once the jets have passed through the gird they collide with each other around the probe. The probe beam passes through the verdet crystal in the center of the two jets before entering the detection system.

tubulent jet then passed through a 1 mm aperture, 0.5 mm thick plastic (ETFE) grid, making the jet turbulent. The magnetic field measurements have been performed in the center of the interaction region, where the jets collide.

The Verdet crystal was held in the center of the colliding jets using an open-ended ceramic tube (outer diameter 2.5 mm, inner diameter 1.3 mm), with the axis of the crystal perpendicular to the incoming jets. The crystal had a diameter of 1 mm and a length of 10 mm. The purpose of the ceramic tube was to protect the Verdet crystal from hard radiation capable of reducing the opacity of the crystal and direct exposure to the plasma flow, as thermal heating can change its birefringence properties[23]. Indeed, we estimate the time taken for heat from the plasma to diffuse through the ceramic tube to be approximately 10 μs, much longer than the duration of the experiment. The probe laser had a power of 100 mW, a wavelength of 532 nm (different from that of the drive beams on the PVDF foils) and was focused with a 1 mm lens to a focal spot of ≈ 0.5 μm. The polarization

of the probe beam was rotated using a half-wave plate to ensure it was at 45° to the optical axis of the beam-splitter before it passed through the crystal.

Figure 2 shows the response of the magneto optical probe in the 1100 ± 10 G test field of a permanent magnet. The field produced by the permanent magnet at the location of the Verdet crystal was measured using a Hall probe. The change in the intensity of each polarization can be seen clearly in Figure 2 (blue lines no field present, red lines field present). The change in rotation angle as calculated using equation 1.3 to be $\Delta\Phi \approx 0.2°$. The magnetic field obtained from equation 1.2 is $\langle B \rangle \approx 1120 \pm 80$ G, in very close agreement to what expected from the Hall probe measurement. While this calibration was done in DC mode, we also expect that the frequency response of the crystal to be uniform over over the range of interest, $f < 100$ MHz.

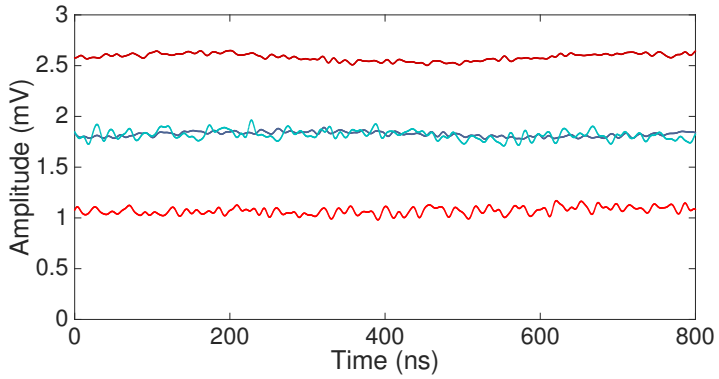

Figure 2. Measurements of the light intensity in both the horizontal and vertical polarizations. The dark and light blue lines show the intensity of each polarization when no magnetic field is present. The dark and light red lines show the intensity of each polarization in the presence of a 1100 G permanent magnetic field.

When operated in the experiment, a optical line filter with a FWHM ≈ 1 nm was used to block any stray light from the target before the probe beam was divided by a 50/50 polarizing beam splitter; each polarization was then detected separately having been focused onto a 2 GHz (DET0.25A Thorlabs) photo-diode connected to a 1 GHz Lecroy oscilloscope.

For comparison the magneto-optic probe was removed and replaced by the induction coil. The B-dot probe is a single axis probe with a single-turn coil with an effective area of 0.29 mm^2 protected by a 2.5 mm diameter glass tube. The coil was oriented such as to measure a symmetrically equivalent component of the magnetic field, that is the component of the magnetic field perpendicular to the bulk flow direction. The design and calibration of the probe has been described by Everson[13]. Calibration of the B-dot with a network analyzer determined the frequency resolution of probe to be 40 MHz. The B-dot probe was connected to the same 1 GHz oscilloscope as used in the Verdet setup.

The jet velocity is found using Schlieren imaging, the electron density from optical interferometry and the electron temperature is determined from emission spectroscopy [24]. These will be briefly discussed below.

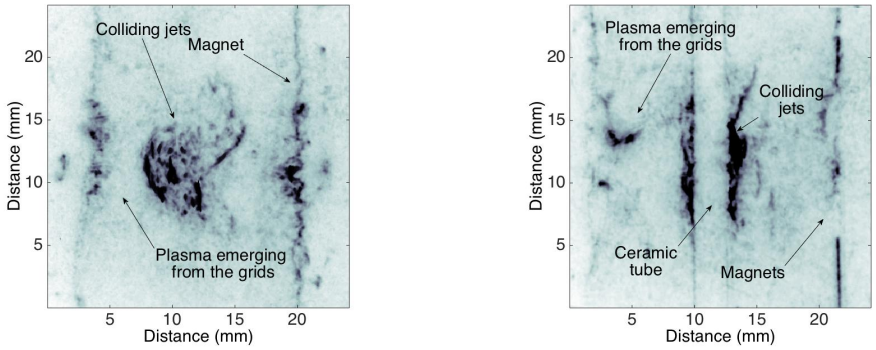

Figure 3. Schlieren images of the collision area. The magnets can be seen at the sides of the image. Plasma is seen emerging from the grids, bordering the magnets. The collision of the two turbulent jets appears in the center of the image ($n_e \approx 10^{18}\,\mathrm{cm}^{-3}$). a) The turbulent plasma 700 ns after the collision (no Verdet probe present). b) The turbulent plasma around the Verdet probe 1000 ns after the collision.

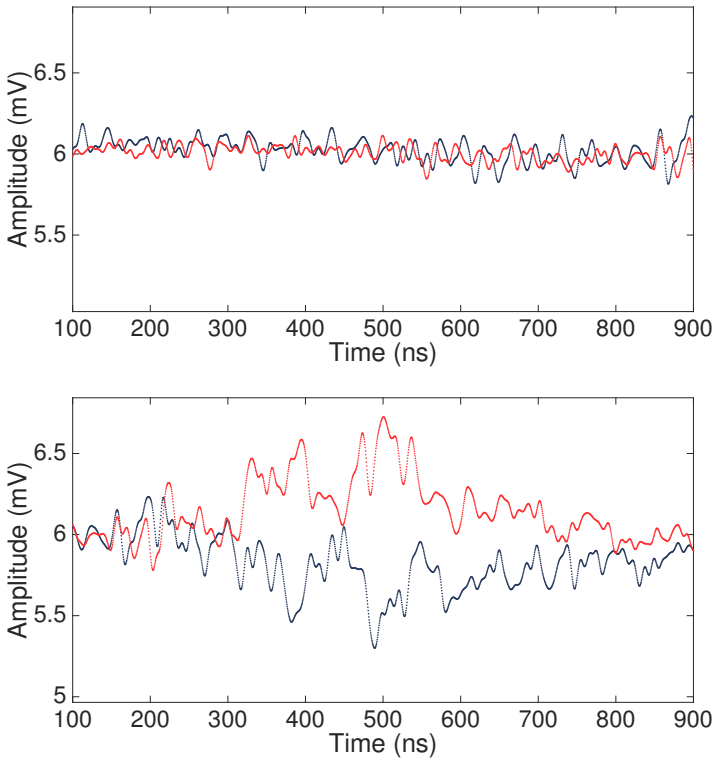

Figure 4. Measurements of the light intensity in both the horizontal (dark blue) and vertical (red) polarizations over 900 ns. a) no magnetised plasma around the probe (before the drive beams fired). b) In the presence of a single plasma jet.

3 Results

Figure 3 shows Schlieren images of the colliding turbulent jets at 700 ns and 1000 ns after the drive beams have fired. The collision of the jets can be seen in the center of the image. At the sides the

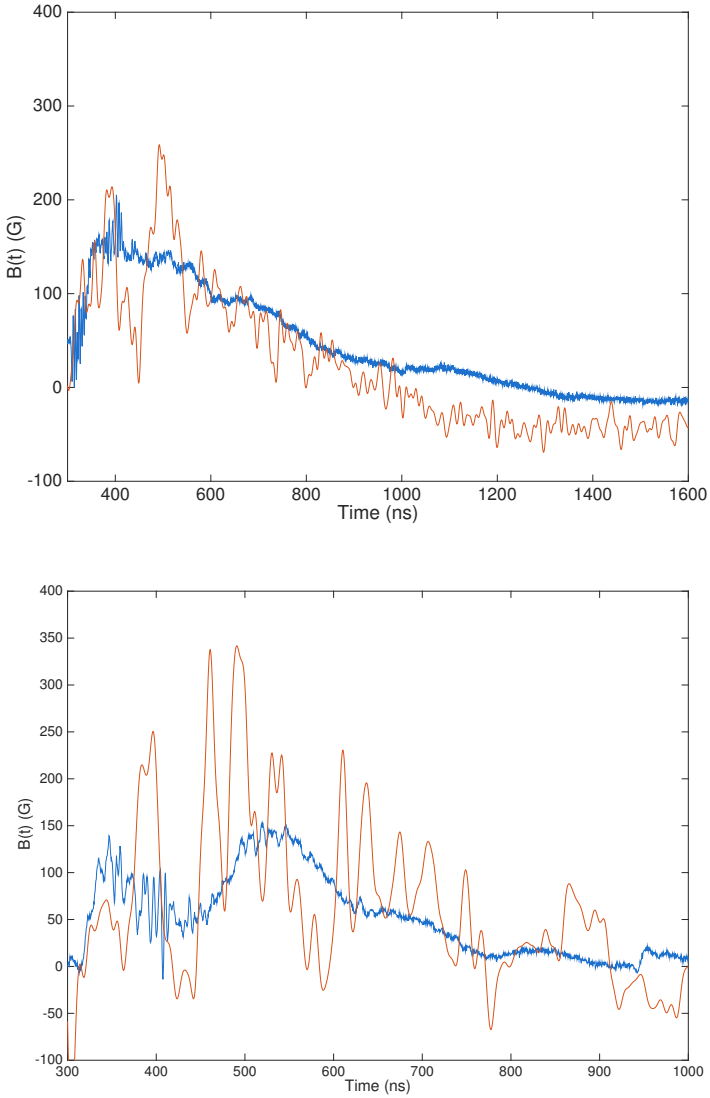

Figure 5. The blue line shows the magnetic field measured by the B-dot probe and the orange line shows the magnetic field measured by the magneto-optic probe. a) A measurement taken for a single jet that has not passed through a grid. b) A measurement taken for two colliding, turbulent jets as the plasma collides and stagnates around the probe.

plasma can be seen emerging from the grids. In figure 3b we also see the outline of the ceramic tube enclosing the Verdet crystal. From the schlieren image we find the turbulent plasma region has a volume of ≈ 1 cm^{-3}. The electron density is $\approx 10^{18}$ cm^{-3} and the electron temperature is ≈ 4 eV during the collision. It is clear from the images that the plasma is turbulent and remains around the probe for at approximately 600 ns after the collision.

Figure 4 shows the intensity of the measured polarizations over a 900 ns period both before the plasma jet arrives at the probe (a) and in the presence of a single plasma jet (b). When no magnetic

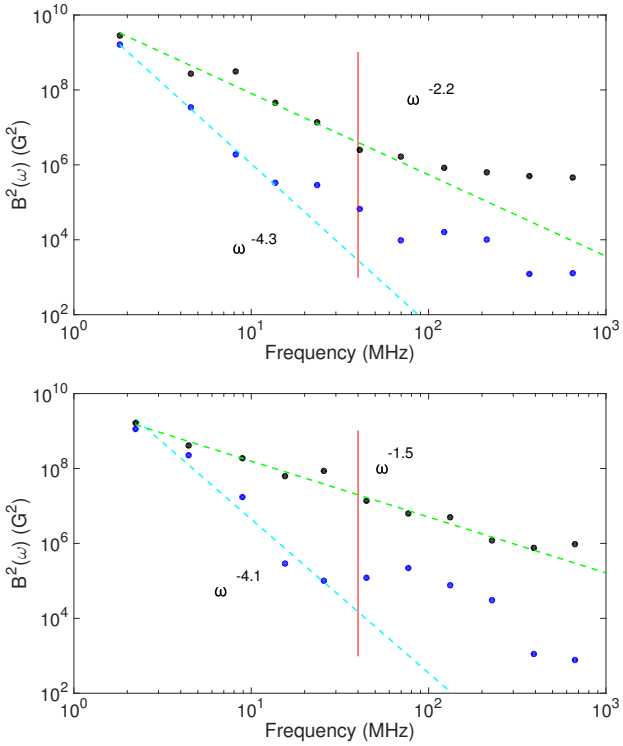

Figure 6. The magnetic power spectra as a function of the frequency for both the B-dot (black markers) and magneto-optic (blue markers) probes. Power laws are fitted to the measured spectra. The red line shows the bandwidth of the B-dot probe. a) Spectra for a single jet. b) Spectra for the collision of two turbulent jets.

field is present the intensity of each polarization arriving at the diode is the same. In the presence of the magnetized plasma the polarization of the light is rotated through the verdet crystal. The magnetic field calculated from these polarizations are shown in figure 5a.

Figure 5 shows the measured magnetic field intensity over the course of the experiment for both a single jet (a) and the collision of two turbulent jets (b). In both cases the field measured by the Verdet and the B-dot probes is similar, although the Verdet measurement shows larger-amplitude oscillations than the B-dot probe, particularly between 300 and 900 ns. Peak values of the magnetic fields are similar $B \approx 200$–300 G. From the noise levels measured before the probe is fired the minimum detectable magnetic field is 30 G. However, it should be pointed out that the magnetic field measured by the Verdet crystal is averaged over the length of the crystal (see introduction), while in the case of the B-dot the field measurement occurs locally in the collision center. Whilst intuitively it would appear that the time-varying magnetic field should be smoother for a measurement integrated along a line of sight (i.e. the Verdet probe) than for the corresponding measurement made at a single point, this is not seen in the data. It is clear from the Schlieren data (see Figure 3) that for both a single jet and a turbulent plasma the spatial structure of the plasma density varies significantly over the length of the crystal. As the field from the permanent magnets is at least partly advected along with the plasma flow, an anisotropic density distribution suggests there will also be a inhomogeneous magnetic field. The difference between the two probe measurements are likely due to the inhomogeneity and anisotropy of the plasma. Figure 6 shows the magnetic

power spectra, $|B(\omega)|^2$ against $\omega/2\pi$ for the fields shown in figure 5. The bandwidth of the B-dot probe, $\sim$ 40 MHz, is highlighted in the figure. The time resolution of the magneto-optic probe in the experiment is limited by the (low) intensity of the probe laser light reaching the photo-diodes, primarily due to the difficulty in focusing through the 1 mm diameter crystal. The bandwidth of the magneto-optical probe was determined to be $\sim$ 100 MHz (set by the noise level), comparable to the B-dot one. Indeed, in Figure 6 we notice that the signal flattens between 60–100 MHz, indicating the start of the noise floor. A power law has been fitted to the linear part of the spectra, giving $\omega^{-4.3}$ and $\omega^{-4.1}$ for the B-dot case, and $\omega^{-2.2}$ and $\omega^{-1.5}$ for the Verdet measurement.

In order to explain these differences, let us assume that, at any given time t, the magnetic field at a point ℓ_0 is related to the magnetic field at a point ℓ along the axis of the TGG crystal by a relation

$$B(t, \ell) \sim B(t, \ell_0)\ell^p, \tag{3.1}$$

where ℓ_0 can be assumed to be the center of the Verdet crystal, where the B-dot measurement is taken, and p is a constant to be determined. From equations (1.2-3.1), we obtain

$$\langle B(t)\rangle \sim B(t, \ell_0)\ell^{p+1}. \tag{3.2}$$

Now, the power spectrum of the magnetic field measured at position ℓ_0 (as obtained from the B-dot data) is

$$M_0(\omega)\omega \sim |B(t, \ell_0)|^2 \sim \omega^{-\alpha+1}, \tag{3.3}$$

with α = 4.1–4.3. The power spectrum of the magnetic field integrated along ℓ (as obtained from the Magneto-optic probe data) is

$$M(\omega)\omega \sim \langle B(t)\rangle^2 \sim |B(t, \ell_0)|^2\ell^{2(p+1)} \sim \omega^{-\beta+1}. \tag{3.4}$$

As the mean flow velocity in the plasma is larger than the velocity fluctuations, then, according to Taylor's hypothesis [25], $\ell \sim t \sim 1/\omega$. As a result of this proportionality relation, $\beta = \alpha + 2(p + 1)$. Since the measurement gives β = 1.5–2.2, we deduce that $p \sim -2$. That is, the magnetic field has a real space distribution as

$$B(t, \ell) \sim \frac{B(t, \ell_0)}{\ell^2}, \tag{3.5}$$

indicating that the magnetic field rapidly decays away from the central region. This shows that the combination of Verdet and B-dot measurements can retrieve important information on both the temporal and spatial structure of the magnetic field.

4 Summary

A probe based on optical Faraday rotation has been used to measure the time-dependent magnetic field in a jet and in a collision between turbulent jets. In both cases the measured fields and spectra were compared to measurements taken by a magnetic induction probe. We show that the two measurements yield identical results if the magnetic field is assumed to rapidly decay away from the center of the interaction region. The principle benefit of a magneto-optic probe over the magnetic induction probe is it's improved bandwidth, as is demonstrated in figure 6.

Acknowledgments

This work was supported by the Engineering and Physical Sciences Research Council (grant numbers EP/M022331/1 and EP/N014472/1), the Science and Technology Facilities Council of the United Kingdom, and by AWE plc.

References

[1] A. A. Schekochihin and S. C. Cowley, *Turbulence, magnetic fields, and plasma physics in clusters of galaxies*, *Physics of Plasmas* **13** (2006) , [0601246].

[2] D. Ryu, H. Kang, J. Cho and S. Das, *Turbulence and Magnetic Fields in the Large-Scale Structure of the Universe*, *Science* **320** (2008) 909—-, [0805.2466].

[3] E. G. Zweibel and C. Heiles, *Magnetic fields in galaxies and beyond*, 1997. 10.1038/385131a0.

[4] A. Marcowith, A. Bret, A. Bykov, M. E. Dieckman, L. O. Drury, B. Lembège et al., *The microphysics of collisionless shock waves.*, *Reports on progress in physics. Physical Society (Great Britain)* **79** (2016) 046901, [1604.00318].

[5] R. J. van Weeren, H. J. A. Röttgering, M. Brüggen and M. Hoeft, *Particle acceleration on megaparsec scales in a merging galaxy cluster*, *Science* **330** (2010) 347, [1010.4306].

[6] R. Blandford and D. Eichler, *Particle acceleration at astrophysical shocks: A theory of cosmic ray origin*, *Physics Reports* **154** (1987) 1–75.

[7] N. L. Kugland, D. D. Ryutov, P.-Y. Chang, R. P. Drake, G. Fiksel, D. H. Froula et al., *Self-organized electromagnetic field structures in laser-produced counter-streaming plasmas*, *Nature Physics* **8** (2012) 809–812.

[8] H. S. Park, C. M. Huntington, F. Fiuza, R. P. Drake, D. H. Froula, G. Gregori et al., *Collisionless shock experiments with lasers and observation of Weibel instabilities*, *Physics of Plasmas* **22** (2015) .

[9] G. Gregori, A. Ravasio, C. D. Murphy, K. Schaar, A. Baird, A. R. Bell et al., *Generation of scaled protogalactic seed magnetic fields in laser-produced shock waves*, *Nature* **481** (2012) 480–483.

[10] J. Meinecke, H. Doyle, F. Miniati and A. Bell, *Turbulent amplification of magnetic fields in laboratory laser-produced shock waves*, *Nature Physics* **10** (2014) 2–6.

[11] J. Meinecke, P. Tzeferacos, A. Bell, R. Bingham, R. Clarke, E. Churazov et al., *Developed turbulence and nonlinear amplification of magnetic fields in laboratory and astrophysical plasmas*, *Proceedings of the National Academy of Sciences* **112** (2015) 8211–8215, [arXiv:1408.1149].

[12] C. Niemann, W. Gekelman, C. G. Constantin, E. T. Everson, D. B. Schaeffer, A. S. Bondarenko et al., *Observation of collisionless shocks in a large current-free laboratory plasma*, *Geophysical Research Letters* **41** (2014) 7413–7418.

[13] E. T. Everson, P. Pribyl, C. G. Constantin, A. Zylstra, D. Schaeffer, N. L. Kugland et al., *Design, construction, and calibration of a three-axis, high-frequency magnetic probe (B-dot probe) as a diagnostic for exploding plasmas*, *Review of Scientific Instruments* **80** (2009) 1–8.

[14] F. C. Jahoda, F. L. Ribe and G. A. Sawyer, *Zeeman-effect magnetic field measurement of a high-temperature plasma*, *Physical Review* **131** (1963) 24–29.

[15] E. a. McLean, J. a. Stamper, C. K. Manka, H. R. Griem, D. W. Droemer and B. H. Ripin, *Observation of magnetic fields in laser-produced plasma using the Zeeman effect*, *Physics of Fluids* **27** (1984) 1327.

[16] I. H. Hutchinson, *Principles of Plasma Diagnostics: Second Edition*, *Plasma Physics and Controlled Fusion* **44** (2002) 2603–2603, [arXiv:1011.1669v3].

[17] J. O. Stenflo, *The Hanle effect and the diagnostics of turbulent magnetic fields in the solar atmosphere*, *Solar Physics* **80** (1982) 209–226.

[18] R. Presura, *Hanle effect as candidate for measuring magnetic fields in laboratory plasmas*, *Review of Scientific Instruments* **83** (2012) .

[19] S. E. Clark, D. B. Schaeffer, A. S. Bondarenko, E. T. Everson, C. G. Constantin and C. Niemann, *Magnetic field measurements in low density plasmas using paramagnetic Faraday rotator glass*, *Review of Scientific Instruments* **83** (2012) 1–4.

[20] W. S. Przybysz, J. Ellis, S. C. Thakur, A. Hansen, R. A. Hardin, S. Sears et al., *A magneto-optic probe for magnetic fluctuation measurements*, *Review of Scientific Instruments* **80** (2009) 1–4.

[21] S. Fujioka, Z. Zhang, K. Ishihara, K. Shigemori, Y. Hironaka, T. Johzaki et al., *Kilotesla magnetic field due to a capacitor-coil target driven by high power laser.*, *Scientific reports* **3** (2013) 1170.

[22] A. B. Villaverde, D. A. Donatti and D. G. Bozinis, *Terbium gallium garnet Verdet constant measurements with pulsed magnetic field*, *Journal of Physics C: Solid State Physics* **11** (2001) L495—-L498.

[23] N. P. Barnes and L. B. Petway, *Variation of the Verdet constant with temperature of terbium gallium garnet*, 1992. 10.1364/JOSAB.9.001912.

[24] T. White, *Super Sonic and Super-Alfvenic Plasma Turbulence. In preperation*, .

[25] M. Wilczek, H. Xu and Y. Narita, *A note on Taylor's hypothesis under large-scale flow variation*, *Nonlinear Processes in Geophysics* **21** (2014) 645–649.